International Journal of GEOMATE, July, 2024 Vol.27, Issue 119, pp.10-17
ISSN: 2186-2982 (P), 2186-2990 (O), Japan, DOI: https://doi.org/10.21660/2024.119.4000
Geotechnique, Construction Materials and Environment

TSUNAMI RUN-UP MODELLING IN COMPARISON WITH COASTAL VULNERABILITY MAPPING

*Abu Bakar Sambah[1,2], Luh Made Sri Masnagari[1], Mochamad Arif Zainul Fuad[1,2], and Candra Adi Intyas[1]

[1]Faculty of Fisheries and Marine Science, Universitas Brawijaya, Indonesia;
[2]Marine Resources Exploration and Management Research Group, Universitas Brawijaya, Indonesia;

*Corresponding Author, Received: 30 June 2023, Revised: 1 Oct. 2024, Accepted: 28 April 2024

ABSTRACT: Tsunami disaster mitigation is essential to reduce the possibility of negative impacts on human life by using ecologically acceptable alternatives. In line with the mitigation efforts, it is essential to focus on strategies such as reducing the risk of casualties and planning for coastal development. An effective method includes the implementation of coastal risk mapping for tsunami disasters. Therefore, this study aimed to determine the propagation and run-up modeling of tsunami waves, as well as evaluate the timing and extent of inundation, and identify affected areas, providing basic information for mapping tsunami risk and vulnerability. Geospatial analysis adopting stacking methods with integrated weighting was applied, using physical topography data as a basis. The results showed that the fault from the earthquake scenario, triggering a tsunami, led to elevated water levels in the southern area. This was attributed to the upward orientation of the fault in the southern area, causing higher waves. Specifically, wave height in the southern area reached a maximum of 8 meters, with the minimum wave value recorded at −4. Tsunami modeling presented a height of 22 meters, resulting in a run-up affecting an area of 965.96 Ha. In conclusion, this study provided an important contribution to the development of the basic theory related to the tsunami risk and vulnerability model.

Keywords: Tsunami, Run-up, Coastal, Vulnerability, Risk

1. INTRODUCTION

Geologically, the southern coast of Java Island is at the confluence of 2 significant plates, namely Eurasian and Indo-Australian. The dynamic interplay of these plates in the area poses a seismic threat, potentially leading to earthquakes capable of triggering tsunamis. A historical account of the events, spanning from 1991 to 2006, as documented by the Indonesian Agency for Meteorological, Climatological, and Geophysics, shows a significant incident. On June 3, 1994, a tectonic earthquake in the Indian Ocean, registering a magnitude of M = 7.8, instigated a tsunami along the southern coast of East Java, resulting in extensive damage to coastal settlements, particularly in the southern coastal area of Banyuwangi Regency, with an estimated death toll of 215 people [1]. Based on the recurrence of earthquake-tsunami events over a prolonged period, there exists the potential for similar incidents in coastal areas of East Java.

In late 2016, an earthquake at the bottom of the waters presented the looming threat of tsunami waves in coastal areas of East Java. This incident served as a warning, presenting the vulnerability of the southern region of Java Island, especially the southern part of East Java, to tsunami risks. According to the USGS (United States Geological Survey) earthquake risk program, a magnitude 5.7 earthquake occurred in the southern waters of East Java on November 16, 2016, at 15:10:10 UTC. This event was experienced simultaneously on 3 islands, namely Java, Bali, as well as Lombok, and had epicenter at coordinates 9.39° S and 113.09° E, the forearc basin of the Indian Ocean, approximately 165 km southeast of Malang, East Java, and at a depth of 85 km [2].

The focus of tsunami disaster mitigation is to reduce the potential negative impacts on life by adopting ecologically acceptable alternatives. This comprises efforts to reduce risk of casualties and strategic planning for coastal development. A crucial aspect of the mitigation includes mapping the vulnerability of coastal areas to tsunami disasters, to reduce risk of life loss.

The development of remote sensing technology using satellite photos, supported by geo-spatial analysis in the concept of multi-criteria analysis, has significantly contributed to comprehensive studies. These studies play an essential role in estimating regional vulnerability to tsunami disasters and assessing tsunami risk. The Cornell Multi-grid Coupled Tsunami Model (COMCOT) software, developed by Professor Philip Liu, has proven instrumental. It is an open-source tool that applies equations of wavelengths and shallow waters through numerical simulations [3]. Numerical modeling is usually used to identify inundation areas by generating a map serving as a

reference for identifying tsunami-prone areas [4].

A previous study applied remote sensing and spatial multi-criteria analysis to evaluate tsunami vulnerability in the coastal area of Miyagi Prefecture, Japan [5]. Similarly, some reports on tsunami vulnerability incorporated remote sensing in risk and vulnerability assessment related to ecological and socio-economic vulnerability. Methods such as moderate-resolution optical satellite images, Digital Elevation Model, and integrated GIS analyses have been applied to identify inundation areas due to tsunamis [6, 7, 8]. Furthermore, parameters including soil type, urban form, and social factors have played a key role in determining tsunami-vulnerable areas. This determination is often achieved by comparing the building damage map with the topography data [9]. A numerical model of tsunami inundation has been developed, and an upscaled urban roughness parameterization and Drag Force Model (DFM) have been validated. This model stimulates the effect of structures as a drag force acting on flow, including multi-physics simulations for source modeling, risk assessment, as well as real-time forecasting and warning [10, 11].

To reduce the risk of coastal disasters, conducting a risk mapping study is essential for predicting and mapping potentially affected areas. This investigation aims to show the propagation of tsunami waves (ocean modeling) and run-up (run-up modeling). It also evaluates the timing of propagation and extent of inundation and identifies the affected areas. Additionally, the study analyzes physical parameters to map risk areas associated with tsunami disasters.

2. RESEARCH SIGNIFICANCE

This study aims to identify areas prone to inundation in the event of a tsunami. Additionally, mapping areas with high vulnerability serves as crucial data for planning effective evacuation routes. By analyzing tsunami potential run-up, inundation, and vulnerability, a mitigation plan can be implemented to reduce the impact of tsunami disasters. The areas with potential tsunami inundation are designated as priority zones for evacuation. Both evacuation routes and buildings are planned in areas distant from tsunami inundation and fall outside the high-risk category.

3. METHODS

3.1 Study Area and Dataset

This study was conducted in the coastal area of Benoa, Bali, as presented in Fig 1. Benoa is a key tourist attraction in Bali. Geographically situated in the eastern part of Benoa Bay, it faces the Indian Ocean to the southern area. Historical data indicates that tsunamis have occurred 3 times in the southern area of Bali. These incidents occurred during significant seismic events, namely the 'Gejer Bali' earthquake on January 21, 1917, the Sumba earthquake with a magnitude of 8.3 on August 19, 1977, and the Banyuwangi earthquake with a magnitude of 7.8 on June 2, 1994.

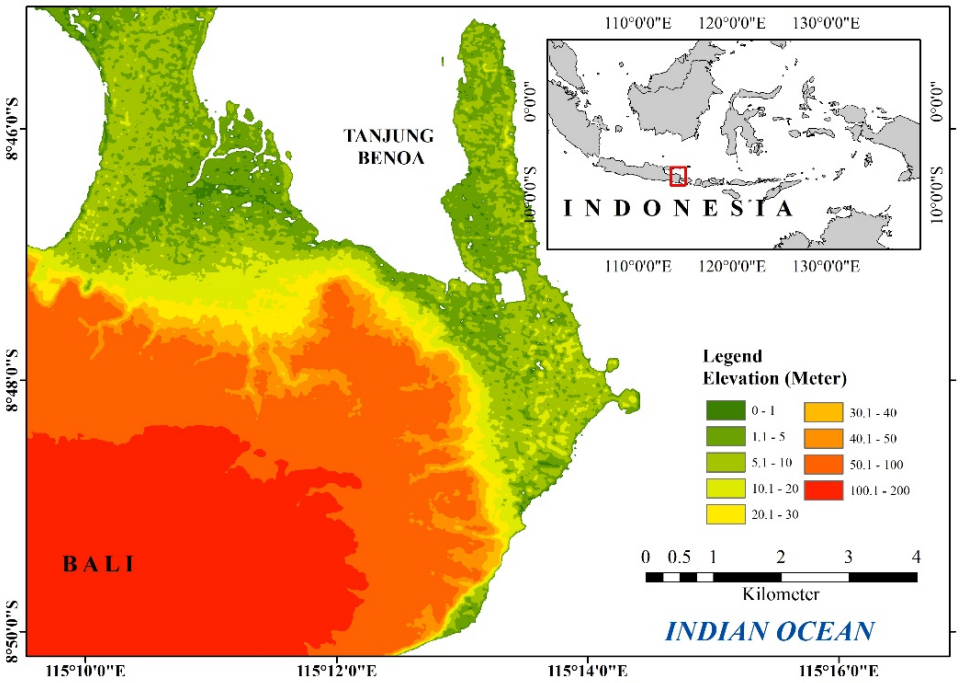

Fig 1. Study area (Benoa, Bali)

Data collected for the analysis were utilized to address the objectives of the study. Table 1 shows

the data and sources of acquisition.

Table 1 Dataset

No	Data
1	Simulation Script, as a command algorithm for running the simulation. Source: https://github.com/AndybnAC T/GPU-comcot/commit/
2	Digital Elevation Model (DEM) for the elevation and slope analysis in the physical tsunami vulnerability mapping. Source: https://tanahair.indonesia.go.id/demnas/
3	Bathymetry, to identify the depth and topography of the waters. Source: https://www.gebco.net
4	Earthquake historical data, as an input parameter for the simulation. Source: National Center for Earthquake Studies 2017
5	Landsat 8 OLI, for the landcover mapping. Source: https://www.usgs.gov

3.2 Tsunami Modelling

Tsunami modeling data processing was conducted using COMCOT v1.7 software. These yielded results pertaining to the height and travel time of the tsunami upon reaching the land, as well as the initial conditions during an earthquake. The parameters used in this study were sourced from the National Center for Earthquake Studies, with fault parameters obtained from the Indonesian Agency for Meteorological, Climatological, and Geophysics. The investigation considered the worst scenario, including focal depth, length, width, dislocation, strike angle, dip angle, slip, origin numerical domain, and epicenter, as shown in Table 2.

The script will be executed through the command prompt, which generates output from COMCOT v1.7. The file COMCOT.CTL comprises all parameters needed for tsunami simulation with COMCOT. In case multiple fracture fields are specified, an additional control file is FAULT_MULTI.CTL was required to set the parameters for the fracture fields. The parameter data was subjected to modification or viewing using any TXT modification application, such as WordPad, UltraEdit, and NotePad. It is important to note that the structure of these 2 files should remain unchanged, except for the VALUED FIELD. Any additional alteration may lead to difficulties in COMCOT properly reading the files. In summary, COMCOT.CTL contained 4 parameter sections, offering control over the simulation, namely fault model, wave generator, slide, and grid settings.

Table 2. Geographic coordinate for the data layer

No	Latitude (S)	Longitude (E)	Grid ID
1	-11.8	111.2	01
	-6.2	118.8	
2	-9.1	114.2	02
	-7.53	115.8	
3	-9	114.8	03
	-8.5	115.5	
4	-8.9	115.05	04
	-8.6	115.3	
5	-8.9	115.14	05
	-8.8	115.18	

The earthquake parameter data utilized as input in COMCOT v1.7 adopts the Worst-Case scenario, featuring a magnitude value of 8.5 Mw. The associated parameters are detailed in Table 3.
Information in Table 3:
L = length (length of fault)
W = width (width of fault)
D = dislocation headings should be avoided

3.3 Tsunami Run-Up

In this study, data processing comprised the running of tsunami modeling scenarios to generate wave height. The utilized parameters included focal depth, length, width, dislocation, strike angle, dip angle, slip, origin numerical domain, and epicenter area. Additionally, slope data and land use were other crucial parameters for this study. The modeling results were analyzed using ArcGIS software and combined with other supporting data. This integration aims to determine the height of tsunami run-up by applying the Hloss method.

3.4 Tsunami Vulnerability

Tsunami vulnerability was analyzed using

Table 3. Tsunami modelling parameters

Sub Fault	Sumba Megathrust										
	Epicenter (deg)		Mag.	Depth	Focal Mechanism			Dimension		Disloc.	Rigidity
	Long	Lat	Mw	Km	Strike	Dip	Rake	L(km)	W(km)	(m)	(GPa)
Fault 1	114.14	-9.82	8.15	31	277	19.7	90	108	75	8.687	30
Fault 2	115.14	-9.88	8.22	30	273	18.4	90	108	75	11.076	30
Fault 3	116.14	-9.94	8.18	29.5	274	17.5	90	108	75	9.647	30

elevation, slope, coastal proximity, and land use. The physical parameters were processed in a geospatial analysis format, with calculations based on the criteria outlined in Table 4. These criteria were selected due to their significant influence on determining vulnerability of a given area and were divided into 5 classes. A very high vulnerability class indicated that the area was highly susceptible and would experience the most significant impact in the event of tsunami.

Table 4. Tsunami vulnerability criteria

Elev. (m)	Slope (%)	Coastal prox. (m)	Land use	Class
<5	0-2	<556	Urban	High
5-10	2-6	556-1400	Agriculture	Slightly High
10-15	6-13	1400-2404	Bare land	Medium
15-20	13-20	2404-3528	Water	Slightly Low
>20	>20	>3528	Forest	Low

The entire data were analyzed through an overlay process in the Geographic Information System (GIS) framework. GIS has several components such as layout, graphics, numbers, and textual components [12, 13].

4. RESULT AND DISCUSSION

4.1 Tsunami Modelling and Time Travel

Tsunami wave height, as shown in Fig 2, was divided into 5 classes, namely 0-3m (dark green), 3-6 m (light green), 6-10 m (yellow), 10-14 m (orange), and 14-22 m (red). Based on the elevation, the Benoa area had a low topography, generating the highest wave of 22 meters upon reaching land. In areas near the coastline, a predominant yellow color indicated that tsunami height was 6-10 m on the mainland.

Earthquake source used in this modeling has fault areas listed in Table 5, with a magnitude of 8.5 Mw, influencing the initial sea conditions which are marked in green, as presented in Figure 3. The fault from earthquake resulted in higher water levels in the south position, as it was pointing upwards, contributing to an elevated wave, indicated by yellow with a value reaching 8. In contrast, blue signifies a value of up to -4, reflecting a downward-pointing fault causing water to flow in that direction.

Table 5. Tsunami time travel

No	Sample	Time travel (minute)
1	Point-1	20 minutes
2	Point-2	20 minutes
3	Point-3	5 minutes

Tsunami modeling produces sea level movements that last for 3 hours (10800 seconds). This study showed that the sea conditions near the earthquake epicenter are influenced by both the hypocenter and plate shifts. These factors can influence sea level, leading to rise and fall. In areas adjacent to the sources of marine earthquake (fault), certain sections of the ocean floor will be permanently uplifted, while others subsidized. This phenomenon prompted the up-and-down movement of the water column. The distribution of the maximum amplitude of tsunami can describe the distribution of the impact and the pattern of movement of wave from the epicenter to the mainland.

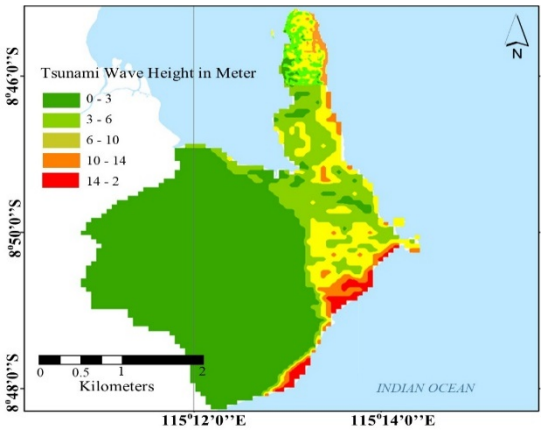

Fig 2. Estimated tsunami wave height map

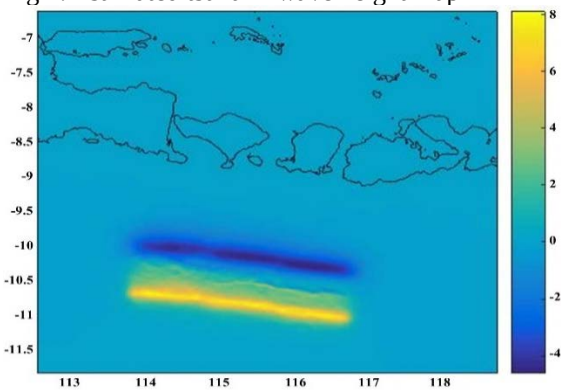

Fig 3. Initial Conditions Immediately after Earthquake

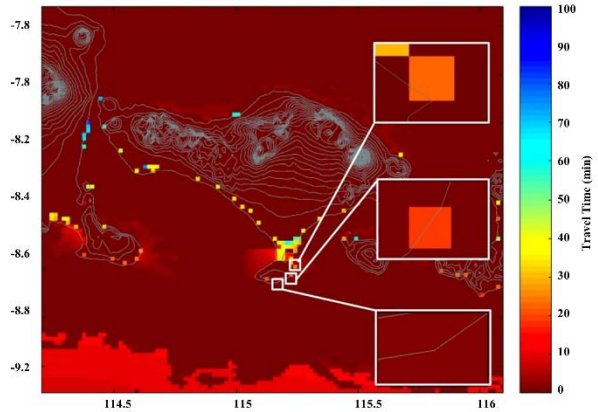

Fig 4. Tsunami time travel

The height of approaching wave was influenced by the slope of the seafloor and coastal cliffs. It is important to note that the slope angle of the cliff affected the rule of tsunami amplification factor, fluctuating with incoming wave. A toe-erosion cliff had a lesser run-up than a typical cliff. Additionally, the length and run-up of an underwater ramp have an interrelated effect [14].

The variances in distance between the observation station and the epicenter accounted for the variations in tsunami travel times. The time taken for wave to reach the land increases with the distance between the observation site and the epicenter. Due to the characteristics of the water and the bathymetry of the sea floor, tsunami wave that reaches the land vary in shape [15].

In the conducted tsunami modeling, run-up map results were obtained according to the height of wave. For instance, in Fig 5(a), showing a tsunami height of 22 meters, the area affected by the run-up was 965.96 Ha. Similarly, a height of 10 m produced the same measurement of the affected area at 965.96 Ha. Another comparison was observed in Fig 5(c), representing a 3 m tsunami, which yielded a run-up area of 179.48 Ha. This variation was attributed to coastal area of Benoa, Bali, characterized by low topography and high levels of tsunami vulnerability.

Table 6. Predicted inundation area

No	Wave height	Run-up area (Ha)
1	22 m	965.96
2	10 m	965.96
3	3 m	179.48

Tsunami inundation is one of the last stages of tsunami evolution, occurring when wave encroaches and floods dry ground, claiming a significant portion of the victims during this stage. The nature of the method, whether a steady and relatively calm rise of the ocean surface, depends on various factors such as wave height, period, and coastline morphology, including beach slope and roughness. The open ocean propagation of a traditional tsunami is a very simple process, transmitting wave energy across basins with fluctuations in wave speed dictated by local depth. Upon reaching the nearshore area, defined by sea depths of 100 m or less, a tsunami is subjected to significant physical modification [16]. In numerical studies, individual wave crests were mostly dispersed, and run-up was dominated by the carrier wave, resulting in a time-dependent, wave setup challenge [17].

In addition to identifying major potential run-up, model results also showed less vulnerable or sheltered areas, such as the southern and eastern of Phuket Island. The model anticipates mild run-up in these areas, ranging from 1 to 2 m, which could be useful for coastal redevelopment plans. However, any rebuilding initiatives would have to be carefully planned, possibly incorporating simulated tsunami risk maps created with even smaller grids, specifically in challenging topography contexts [18].

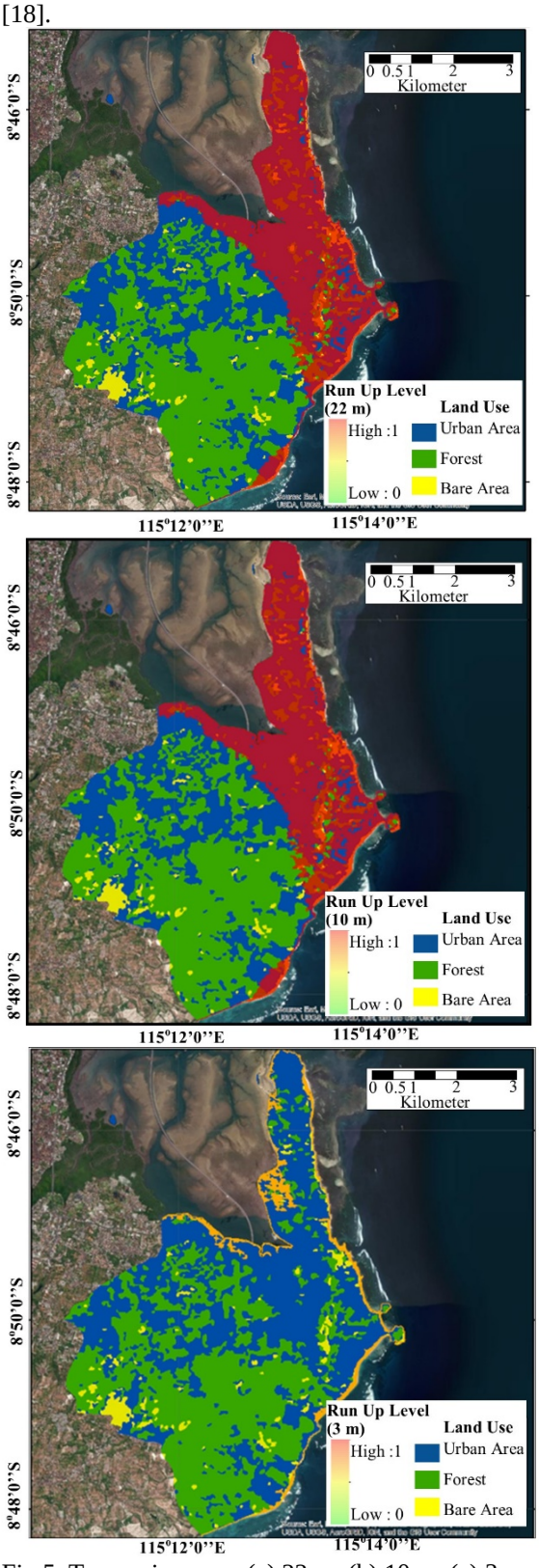

Fig 5. Tsunami run-up; (a) 22 m; (b) 10 m; (c) 3 m,

and in comparison with land use.

4.2 Vulnerability Mapping

The elevation of Benoa Bali coastal area is classified as low with a value of < 5 m (high levels of tsunami vulnerability). Benoa area has a relatively low elevation compared to other areas in southern Bali. Despite hosting numerous tourist attractions and hotels situated along the coast, some parts of this area has relatively higher elevations, ranging from 15-20 m. Areas with low elevations have a higher level of vulnerability to tsunami, as wave easily penetrates land and hits the ground. Conversely, areas with high elevations have a lower level of vulnerability to tsunami. The interplay between low and high elevations in an area significantly influences the extent of run-up.

The slope parameter in Benoa coastal area is classified as sloping with a percentage of 6-13% (high to slightly high levels of tsunami vulnerability). Areas with a gentle slope are vulnerable to tsunami, with the impact increasing as the slope becomes gentler or lower. Steeper or higher slopes result in diminished tsunami wave impact. Based on the field survey, coastal area is densely populated with a gentle slope, contributing to increased tsunami risk.

Using the parameters and classes as shown in Table 4, the map of tsunami vulnerability area was created, as shown in Fig 6. Spatial Multicriteria Analysis (SMCA) helps prioritize the decision-making process through the integration of geo-reference data. This tool is vastly different from conventional multi-criteria decision-making methods, due to the inclusion of an explicit geographic element. In contrast to traditional MCDM analysis, SMCA considers both criterion values and geographical information of criteria, as well as the decision-maker preferences regarding a set of assessment parameters [19, 20]. Physical characteristics, such as elevation, slope, shoreline proximity, and land use, could be used to determine vulnerability maps. Some studies further included coastal geomorphology, coastal ecosystem resources, tsunami wave direction, and distance from the river [21, 22, 23]. The high vulnerability areas were mostly identified in coastal area with the sloping coast type. Furthermore, elevation and slope play an important role in governing the stability of a terrain [24]. A Tsunami vulnerability study in Bali shows the non-uniform distribution of vulnerability, is highly influenced by coastal proximity, elevation, and slope [25, 26].

The places with the most potential for infrastructure destruction, physical harm to the environment, and fatalities were those with high and very high tsunami risk. The area was distinguished by beaches and coastal areas with a gentle slope, lower land elevation, terrestrial vegetation, shrubs, and fields. The proximity to the coastline, the presence of a river, and a relatively dense population further contribute to the increased risk [27].

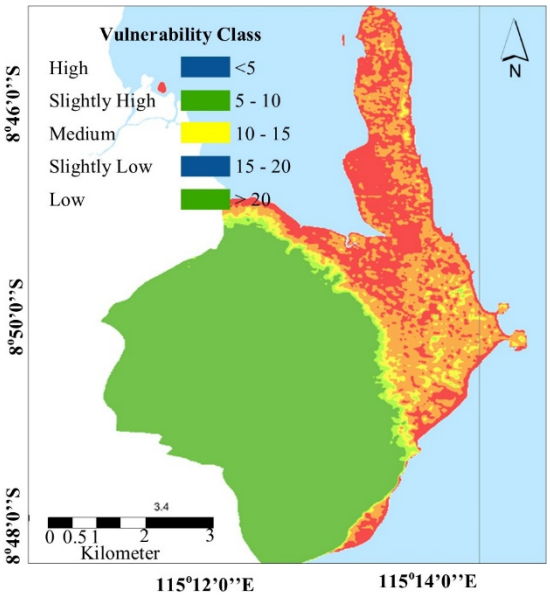

Fig 6. Tsunami vulnerability map

In generating an inundation map derived from tsunami vulnerability map, historical tsunami, and observation data were crucial factors. Predominantly, high vulnerability areas were in line with sloping coasts, and capes, and are predicted to experience inundation, spreading to places identified with high and slightly high vulnerability. Furthermore, in the pairwise comparison, elevation holds the highest weight.

The study from the 2011 Tohoku Earthquake Tsunami Joint Survey Group showed that most of the damage area was dependent on surface elevation. This was substantiated by instances where areas near the coastline but at higher elevations suffered comparatively less damage. Most of the damage occurred on flat surfaces, where tsunami wave had unrestricted flow [28].

5. CONCLUSIONS

In conclusion, tsunami resulting from earthquake was characterized by wave propagation and varying heights. The fault caused a rise in water levels in the southern region, with the southern part pointing upwards, leading to elevation variations between -4 and 8 meters. Tsunami modeling, which used a propagation time of 3 hours, indicated a consistent impact zone irrespective of tsunami height, comprising an area of 965.96 hectares. In

addition, for effective disaster mitigation, the integration of tsunami modeling methods and spatial multicriteria analysis for vulnerability mapping proved to be a valuable method. The modeling outcomes affirmed that areas susceptible to tsunami inundation fell in high and very high vulnerability classes, as determined through geospatial analysis. To minimize damage and loss of life, it was crucial to establish evacuation routes and identify evacuation building areas based on the integration of these two methods. The results of this study served as fundamental information for effective disaster management in coastal areas.

An integrated tsunami risk assessment is essential for comprehensive disaster management. This assessment should comprise risk, vulnerability maps, and tsunami wave propagation models derived from the study. Risk assessment quantifies the possible damage and loss due to tsunami by integrating the results of risk assessment with tsunami vulnerability.

6. ACKNOWLEDGEMENTS

The authors are grateful to the Geospatial Information Agency of Indonesia for the National Digital Elevation Model (DEMNAS) data, and the National Center for Earthquake Studies for earthquake historical data. The authors are also grateful to the Faculty of Fisheries and Marine Science, Universitas Brawijaya, Indonesia, under the scheme of *Hibah Penelitian Doktor Lektor Kepala* 2022, for funding this study.

7. REFERENCES

[1] Synolakis C., Imamura F., Tsuji Y., Matsutomi H., Tinti S., Cook B., Chandra Y.P., and Usman M., Damage, conditions of East Java Tsunami of 1994 analyzed, EOS, Vol. 76, Issue 26, 1995, pp. 257-260.

[2] USGS National Earthquake Information Center. M 5.7 - 80 km S of Kencong, Indonesia, U.S. Geological Survey, 2016, http://earthquake.usgs.gov/earthquakes/eventpage/us100078vh#executive

[3] Pradjoko E., Kusuma T., Setyandito O., Suroso A., and Harianto B., Tsunami Run-up Assessment of 1977 Sumba Earthquake in Kuta, Central of Lombok, Indonesia. 2nd International Seminar on Ocean and Coastal Engineering, Environment and Natura Disaster Management, ISOCEEN 2014, Procedia Earth and Planetary Science 14, 2015, pp. 9-16.

[4] Laksono T.F.X.A., Aditama M.R., Setijadi R., and Ramadhan G., Run-up Height and Flow Depth Simulation of the 2006 South Java Tsunami Using COMCOT on Widarapayung Beach. Conference proceedings, in Proc. IOP Conf. Ser. Mater. Sci. Eng., Vol. 982, 012047, 2020.

[5] Sambah A.B., and Miura F., Remote sensing and spatial multi-criteria analysis for tsunami vulnerability assessment. Disaster Prevention and Management, Vol. 23, Issue 3, 2014, pp. 271 – 295.

[6] Eckert, S., Jelinek, R., Zeug, G. and Krausmann, E., Remote sensing-based assessment of tsunami vulnerability and risk in Alexandria, Egypt. Applied Geography, Vol. 32, No. 2, 2012, pp. 714-723.

[7] Mahendra, R.S., Mohanty, P.C., Bisoyi, H., Kumar, T.S. and Nayak, S., Assessment and management of coastal multi-hazard vulnerability along the Cuddalore Villupuram, east coast of India using geospatial techniques. Ocean & Coastal Management, Vol. 54, No. 4, 2011, pp. 302-311.

[8] Strunz, G., Post, J., Zosseder, K., Wegscheider, S., Muck, M., Riedlinger, T., Mehl, H., Dech, S., Birkmann, J., Gebert, N., Harjono, H., Anwar, H.Z., Sumaryono, Khomarudin, R.M. and Muhari, A., Tsunami risk assessment in Indonesia. Natural Hazards and Earth System Science, Vol. 11, No. 1, 2011, pp. 67-82

[9] Gokon, H. and Koshimura, S., Mapping of building damage of the 2011 Tohoku earthquake tsunami in Miyagi Prefecture. Coastal Engineering Journal, Vol. 54, No. 1, 2012, pp. 126-138.

[10] Fukui N., Prasetyo A., and Mori N., Numerical modeling of tsunami inundation using upscaled urban roughness parameterization. Coastal Engineering, Vol. 152, 2019, 103534,

[11] Sugawara D., Numerical modeling of tsunami: advances and future challenges after the 2011 Tohoku earthquake and tsunami. Earth-Science Reviews, Vol. 214, 2021, 103498.

[12] Worboys M.F., GIS: A Computing Perspective. Published by Taylor & Francis, Bristol, 1995.

[13] Abdul-Rahman A., and Pilouk, M., Spatial Data Modelling for 3D GIS, Springer: New York, 2008

[14] ZhaoX., Chen Y., Huang Z., and Gao Y., A numerical study of tsunami wave run-up and impact on coastal cliffs using a CIP-based model, Nat. Hazards Earth Syst. Sci., Vol. 37, 2017, pp 1-17].

[15] Subardjo P., Saputro S., and Aeda S.A., Simulation of tsunami wave propagation and run-up at Pangandaran Bay, West Java, International Journal of Marine and Aquatic Resource Conservation and Co-existence, Vol. 2, Issue 1, 2017, pp. 31-37]

[16] Lynett P.J., Tsunami Inundation, Modeling of. In: Meyers, R. (eds) Encyclopedia of Complexity and Systems Science. Springer, New York, 2009.
[17] Korycansky D.G., and Lynett P., Runup from impact tsunami. Geophys J Int, Vol. 170, Issue 3, 2007, pp. 1076–1088.
[18] Ioualalen M., Asavanant J., Kaewbanjak N., Grilli S.T, Kirby J.T, and Watts P., Modeling the 26 December 2004 Indian Ocean tsunami: Case study of impact in Thailand. Journal of Geophysical Research: Oceans, Vol. 12, No. 7, 2007, pp. C07024.
[19] Carver S.J., Integrating Multi-Criteria Evaluation with Geographical Information Systems. International Journal of Geographical Information Systems, Vol. 5, No. 3, 1991, pp. 321-339.
[20] Jankowski P., Integrating Geographical Information Systems and Multiple Criteria Decision-Making Methods. International Journal of Geographical Information Systems, Vol. 9, Issue 3, 1995, pp. 251-273.
[21] Papathoma M., and Dominey-Howes D., Tsunami vulnerability assessment and its implications for coastal hazard analysis and disaster management planning, Gulf of Corinth, Greece. Natural Hazards and Earth System Sciences, Vol. 3, Issue 6, 2003, pp. 733–747.
[22] Sengaji E., and Nababan B., Tsunami risk level mapping in Sikka, East Nusa Tenggara. Journal of Tropical Marine Science and Technology, Vol. 1 No. 1, 2009, pp. 48- 61.
[23] Eddy, GIS in disaster management: a case study of tsunami risk mapping in Bali, Indonesia. Masters (Research) Thesis, James Cook University, Australia, 2006.
[24] Guntur, Sambah A.B., Miura F., Fuad, and Arisandi D.M., Assessing tsunami vulnerability areas using satellite imagery and weighted cell-based analysis. International Journal of GEOMATE, Vol.12, Issue 34, 2017, pp. 115-122
[25] Sambah A.B., and Miura F., Remote sensing and spatial multi-criteria analysis for tsunami vulnerability assessment, Disaster Prevention and Management, Vol. 23, Issue 3, 2014, pp. 271–295.
[26] Sambah A.B., and Miura F., Spatial data analysis and remote sensing for observing tsunami-inundated areas, International Journal of Remote Sensing, Vol. 37, Issue 9, 2016, pp. 2047-2065.
[27] Faiqoh, I., Gaol, J.L., and Ling, M.M., vulnerability level map of tsunami disaster in Pangandaran beach, West Java, International Journal of Remote Sensing and Earth Sciences, Vol.10, No.2, 2013, pp. 90-103.
[28] Asakura R., Iwase K., Ikeya T., Takao M., Kaneto T., Fujii N., and Ohmori M., The tsunami wave force acting on land structures. Conference proceedings, in Proc. the 28th International Conference on Coastal Engineering, 2003, pp.1191-1202.